

# A Spectral Approach to Optimal Control of the Fokker–Planck Equation\*

Dante Kalise<sup>1</sup>, Lucas M. Moschen<sup>1</sup>, Grigorios A. Pavliotis<sup>1</sup> and Urbain Vaes<sup>2</sup>

**Abstract**—In this paper, we present a spectral optimal control framework for Fokker–Planck equations based on the standard ground state transformation that maps the Fokker–Planck operator to a Schrödinger operator. Our primary objective is to accelerate convergence toward the (unique) steady state. To fulfill this objective, a gradient-based iterative algorithm with Pontryagin’s maximum principle and Barzilai–Borwein update is developed to compute time-dependent controls. Numerical experiments on two-dimensional ill-conditioned normal distributions and double-well potentials demonstrate that our approach effectively targets slow-decaying modes, thus increasing the spectral gap.

## I. INTRODUCTION

Optimal control of diffusion processes, whose dynamics are modeled by Fokker–Planck equations (FPEs), arises in a wide range of applications, from molecular dynamics [3] and optics [15] to social phenomena such as pedestrian movement [12], opinion formation ([2], [10]), and wealth distribution [19]. By designing controls that act on the FPE, one can steer the probability distribution toward a desired state, accelerate convergence to equilibrium, or stabilize otherwise slow-mixing dynamics. Developing efficient approaches for this purpose supports tasks ranging from targeted sampling to population-level coordination and is at the heart of our investigation in this paper.

In controlling the FPE, first- and second-order optimality conditions have been derived for an optimal control problem [5]. Meanwhile, infinite-horizon control strategies have been proposed for overdamped Langevin dynamics to stabilize the FPE and enhance convergence to the stationary (Gibbs) measure [9]. This is especially relevant to sampling, where optimal Langevin samplers improve mixing by modifying the drift term of the associated SDE [16] by designing the control input appropriately. A discussion of the FP control framework, including its formulation for various FP equations and its connection to dynamic programming, can be found in [4].

Building on these ideas, we employ a spectral-numerical method to develop systematic and efficient control methodologies for the FPE. Specifically, this paper proposes an optimal

control framework to accelerate the convergence of the Fokker–Planck equation toward its steady-state distribution, which is assumed to be unique. Although our broader objectives encompass mean-field-type PDEs, we focus on the linear FPE as a fundamental case study, presenting both the theoretical foundation and numerical results.

Unlike finite-volume or finite-difference discretizations, spectral methods rely on eigenfunction expansions to approximate solutions accurately while maintaining low computational cost. This approach is especially advantageous in unbounded domains, where conventional grid-based methods struggle. In addition, spectral formulations naturally connect to Schrödinger-type transformations of the Fokker–Planck operator, enabling direct use of techniques from quantum mechanics and numerical linear algebra [20]. This link was successfully exploited in multiscale stochastic differential equations, demonstrating the versatility of spectral approaches [1].

The main contributions of our paper are:

- We extend the Hermite-based approach of [18] to a broader class of non-quadratic potentials.
- We derive the state–adjoint optimality system for the control problem and propose a gradient-based iterative algorithm (employing Barzilai–Borwein updates) to compute the optimal control.
- We introduce a strategy for choosing the control shape functions to target the slow-decaying spectral modes, and we demonstrate via numerical experiments on quadratic and double-well potentials that our method accelerates convergence toward the steady state.

The remainder of this paper is structured as: **Section II** provides a theoretical background on the Fokker–Planck equation and the Schrödinger operator. **Section III** formulates the optimal control problem. **Section IV** presents our numerical approach, detailing the spectral discretization. Finally, **Section V** provides numerical experiments.

*Notation.* We denote by  $L^2(\mathbb{R}^d)$  the space of square-integrable functions with respect to the Lebesgue measure. For a given probability density  $\mu$  on  $\mathbb{R}^d$ , we say that  $\phi$  belongs to the weighted space  $L^2(\mathbb{R}^d, \mu)$  if  $\phi\sqrt{\mu} \in L^2(\mathbb{R}^d)$ . For a given Hilbert space  $(H, \langle \cdot, \cdot \rangle)$ , we denote  $\|\cdot\|_H$  the norm in  $H$  defined through the inner product of  $H$ .

## II. FOKKER–PLANCK EQUATION AND PRELIMINARIES

Consider the diffusion process  $\{X_t\}_{t \geq 0}$  in  $\mathbb{R}^d$  that satisfies the stochastic differential equation

$$dX_t = -\nabla V(X_t) dt + \sqrt{2\sigma} dW_t, \quad (1)$$

\*DK is partially supported by the EPSRC Standard Grant EP/T024429/1. LM is supported by the CNRS-ICL PhD Studentship program. GP is partially supported by an ERC-EPSRC Frontier Research Guarantee through Grant No. EP/X038645, ERC Advanced Grant No. 247031 and a Leverhulme Trust Senior Research Fellowship, SRF\R1\241055. UV is partially supported by the European Research Council (ERC) under the EU Horizon 2020 program (grant agreement No 810367) and by the Agence Nationale de la Recherche under grants ANR-21-CE40-0006 (SINEQ) and ANR-23-CE40-0027 (IPSO).

<sup>1</sup>DK, LMM, and GAP are with the Department of Mathematics, Imperial College, London, UK {d.kalise-balza, lmm122, pav}@ic.ac.uk

<sup>2</sup>UV is with Inria, Paris, France urbain.vaes@inria.fr

where  $V: \mathbb{R}^d \rightarrow \mathbb{R}$  is a potential function,  $\sigma > 0$  is the diffusion coefficient, and  $\{W_t\}_{t \geq 0}$  denotes a standard  $d$ -dimensional Brownian motion. The evolution of the probability density function (PDF)  $\rho(x, t)$  of  $X_t$  is governed by the forward Fokker–Planck equation

$$\partial_t \rho = \mathcal{L}^* \rho, \quad (2)$$

with the initial condition  $\rho(x, 0) = \rho_0(x)$ , which represents the Lebesgue density function of  $X_0$ , satisfying  $\rho_0 \geq 0$ ,  $\int_{\mathbb{R}^d} \rho_0(x) dx = 1$ , and  $\rho_0 \in C^\infty(\mathbb{R}^d)$ . The operator  $\mathcal{L}^*: L^2(\mathbb{R}^d, \rho_\infty^{-1}) \rightarrow L^2(\mathbb{R}^d, \rho_\infty^{-1})$  is defined as

$$\mathcal{L}^* \phi := \nabla \cdot (\phi \nabla V) + \sigma \Delta \phi.$$

We assume that  $V \in C^\infty(\mathbb{R}^d)$  and that

$$\lim_{|x| \rightarrow \infty} V(x) = \infty, \text{ and } e^{-V(\cdot)/\sigma} \in L^1(\mathbb{R}^d)$$

for all  $\sigma > 0$ . Under these assumptions, the PDE is well-posed (see [18, Thm. 2], [20, Thm. 4.2], [9, Prop. 2.1]) and admits a unique stationary density

$$\rho_\infty(x) := Z^{-1} e^{-V(x)/\sigma},$$

where  $Z := \int_{\mathbb{R}^d} e^{-V(x)/\sigma} dx$  [20, Prop. 4.6].

Next, we define

$$W(x) := \frac{1}{4\sigma} |\nabla V(x)|^2 - \frac{1}{2} \Delta V(x) \quad (3)$$

and assume that  $\lim_{|x| \rightarrow \infty} W(x) = \infty$ . Then  $\rho_\infty$  satisfies a Poincaré inequality with a constant  $\lambda > 0$  [7, Cor. 1.6]; in particular, if  $\rho_0 \in L^2(\mathbb{R}^d, \rho_\infty^{-1})$ ,

$$\|\rho(\cdot, t) - \rho_\infty\|_{L^2(\mathbb{R}^d, \rho_\infty^{-1})} \leq e^{-\lambda \sigma t} \|\rho_0 - \rho_\infty\|_{L^2(\mathbb{R}^d, \rho_\infty^{-1})}.$$

Under these hypotheses, the *backward* generator  $\mathcal{L}$  associated with (1) is self-adjoint in  $L^2(\mathbb{R}^d, \rho_\infty)$  and has compact resolvent [20, Sec 4.4].

We perform the (ground state) unitary transformation to map the Fokker-Planck operator  $\mathcal{L}^*$  to a *Schrödinger operator* defined in  $L^2(\mathbb{R}^d)$ . Specifically, define the *unitary operator*

$$\mathcal{U}: L^2(\mathbb{R}^d, \rho_\infty^{-1}) \rightarrow L^2(\mathbb{R}^d) \text{ by } (\mathcal{U}\phi)(x) := \frac{\phi(x)}{\sqrt{\rho_\infty(x)}}.$$

Verifying that  $\mathcal{U}$  is an isometric isomorphism with a well-defined inverse is straightforward.

Based on the unitary operator, we define a new operator  $\mathcal{H}$  on  $L^2(\mathbb{R}^d)$  by

$$\mathcal{H} := -\mathcal{U} \mathcal{L}^* \mathcal{U}^{-1},$$

which has the form  $\mathcal{H} = -\sigma \Delta + W(x)$ . The operator  $\mathcal{H}$  is self-adjoint in  $L^2(\mathbb{R}^d)$  and possesses a purely discrete, unbounded spectrum with eigenvalues of finite multiplicity [22, Thm. XIII.67]. Moreover, standard elliptic regularity theory guarantees that its corresponding eigenfunctions are infinitely differentiable.

Under transformation  $\psi := \mathcal{U}\rho$ , the Fokker-Planck PDE transforms to the equation

$$\partial_t \psi = -\mathcal{H}\psi, \quad (4)$$

with initial condition  $\psi(\cdot, 0) = \psi_0 := \mathcal{U}\rho_0$ . Equation (4) resembles a Schrödinger equation with imaginary time. Transforming the Fokker–Planck operator to a Schrödinger operator enables us to consider the problem in the standard  $L^2(\mathbb{R}^d)$  space, rather than a weighted one. In this flat space, the Schrödinger operator is self-adjoint, and its spectral properties can be analyzed using well-established results from the theory of Schrödinger operators.

### III. OPTIMAL CONTROL PROBLEM FORMULATION

We consider that  $X_t$  is subject to an additional conservative force:

$$dX_t = -\nabla V(X_t) dt - \sum_{i=1}^m u_i(t) \nabla \alpha_i(X_t) dt + \sqrt{2\sigma} dW_t.$$

Here  $u_i: [0, T] \rightarrow \mathbb{R}$  are time-dependent controls in  $L^2([0, T])$ , and  $\alpha_i: \mathbb{R}^d \rightarrow \mathbb{R}$  are shape control functions in  $C^\infty(\mathbb{R}^d)$ . The associated Fokker–Planck equation is given by

$$\partial_t \rho = \mathcal{L}^* \rho + \sum_{i=1}^m u_i(t) \mathcal{A}_i^* \rho, \quad (5)$$

where, for  $i = 1, \dots, m$ ,

$$\mathcal{A}_i^* \phi := \nabla \cdot (\phi \nabla \alpha_i(x)).$$

The objective is to determine a pair  $(\rho, \mathbf{u})$  that minimizes the cost functional

$$\begin{aligned} J(\rho, \mathbf{u}) := & \frac{1}{2} \|\rho(\cdot, T) - \rho^\dagger\|_{L^2(\mathbb{R}^d, \rho_\infty^{-1})}^2 + \frac{\nu}{2} \int_0^T |\mathbf{u}(t)|^2 dt \\ & + \frac{\kappa}{2} \int_0^T \|\rho(\cdot, t) - \hat{\rho}\|_{L^2(\mathbb{R}^d, \rho_\infty^{-1})}^2 dt \end{aligned}$$

subject to the constraint that  $\rho$  satisfies equation (5), with  $\mathbf{u}(t) \in \mathbb{R}^m$ ,  $T > 0$ ,  $\nu > 0$ ,  $\kappa > 0$ , and  $\rho^\dagger \in L^2(\mathbb{R}^d, \rho_\infty^{-1})$  is a desired final distribution. We also include a probability distribution  $\hat{\rho}$ . We focus on the case where  $\rho^\dagger = \hat{\rho} = \rho_\infty$ .

Applying the unitary transformation  $\mathcal{U}$  and defining  $\mathcal{N}_i := \mathcal{U} \mathcal{A}_i^* \mathcal{U}^{-1}$ , we transform the system into the controlled (imaginary-time) Schrödinger equation. The problem then reduces to finding a pair  $(\psi, \mathbf{u})$  that minimizes

$$\begin{aligned} J(\psi, \mathbf{u}) := & \frac{1}{2} \|\psi(\cdot, T) - \psi^\dagger\|_{L^2(\mathbb{R}^d)}^2 + \frac{\nu}{2} \int_0^T |\mathbf{u}(t)|^2 dt \\ & + \frac{\kappa}{2} \int_0^T \|\psi(\cdot, t) - \hat{\psi}\|_{L^2(\mathbb{R}^d)}^2 dt \end{aligned} \quad (6)$$

where  $\psi^\dagger := \mathcal{U}\rho^\dagger$  and  $\hat{\psi} := \mathcal{U}\hat{\rho}$ , subject to the controlled equation

$$\partial_t \psi = -\mathcal{H}\psi + \sum_{i=1}^m u_i(t) \mathcal{N}_i \psi. \quad (7)$$

The operator  $\mathcal{N}_i$ , given in explicit form by Proposition 1, acts as a shape modulation on the density  $\psi$  under the control action  $\mathbf{u}$ .

*Proposition 1:* Define  $b_i := \nabla \alpha_i \cdot \nabla \log \sqrt{\rho_\infty}$ . Then, for all  $\phi \in L^2(\mathbb{R}^d)$ ,

$$\mathcal{N}_i \phi = \nabla \cdot (\phi \nabla \alpha_i) + b_i \phi.$$

Moreover, the formal adjoint of  $\mathcal{N}_i$  in  $L^2(\mathbb{R}^d)$  is

$$\mathcal{N}_i^* \phi = b_i \phi - \nabla \alpha_i \cdot \nabla \phi.$$

*Proof:* See the Appendix (page 6). ■

Standard results in infinite-dimensional optimal control (see, e.g., [17, Ch. 3]) guarantee the existence of an optimal control given the coercivity and weak lower semicontinuity of the cost functional, together with the continuity of the control-to-state mapping. In our setting, the quadratic structure of the cost and the compactness of the resolvent of  $\mathcal{H}$  ensure that a minimizing pair  $(\psi^*, \mathbf{u}^*)$  exists in the admissible control space  $L^2(0, T; \mathbb{R}^m)$ . A similar result can be found in [21, Thm. 1]. In this reference, the Schrödinger equation from quantum mechanics (i.e. in “real-time”) is considered. However, the proof is based on the spectral analysis of the elliptic operator and it can be applied directly to our problem.

To solve problem (6)–(7), we consider the first-order optimality conditions. These conditions are derived by introducing a function  $\varphi \in L^2(\mathbb{R}^d)$  as the adjoint variable and forming the augmented Lagrangian

$$\begin{aligned} \mathcal{L}(\psi, \mathbf{u}, \varphi) := & J(\psi, \mathbf{u}) + \int_0^T \left\langle \varphi(\cdot, t), \partial_t \psi(\cdot, t) \right\rangle_{L^2(\mathbb{R}^d)} dt \\ & + \int_0^T \left\langle \varphi(\cdot, t), \mathcal{H} \psi(\cdot, t) - \sum_{i=1}^m u_i(t) \mathcal{N}_i \psi(\cdot, t) \right\rangle_{L^2(\mathbb{R}^d)} dt. \end{aligned} \quad (8)$$

The first-order optimality conditions are then obtained by taking variations with respect to  $\psi$ ,  $\mathbf{u}$ , and  $\varphi$ , and setting the corresponding gradients to zero.

The adjoint variable  $\varphi$  satisfies

$$\begin{cases} \partial_t \varphi = \mathcal{H} \varphi - \sum_{i=1}^m u_i(t) \mathcal{N}_i^* \varphi + \kappa(\psi - \hat{\psi}), \\ \varphi(x, T) = \psi^\dagger(x) - \psi(x, T), \end{cases} \quad (9)$$

with the optimal control given by

$$u_i(t) = \frac{1}{\nu} \langle \varphi, \mathcal{N}_i \psi \rangle_{L^2(\mathbb{R}^d)} = \frac{1}{\nu} \langle \mathcal{N}_i^* \varphi, \psi \rangle_{L^2(\mathbb{R}^d)}, \quad (10)$$

which is obtained by setting the gradient equal to 0:

$$\nabla_{u_i} \mathcal{L} := \nu u_i - \langle \mathcal{N}_i^* \varphi, \psi \rangle_{L^2(\mathbb{R}^d)} = 0. \quad (11)$$

In equation (9), we used that  $\mathcal{H}$  is a self-adjoint operator. Therefore, if there exists an optimal pair  $(\psi^*, \mathbf{u}^*)$ , then this pair satisfies equations (7), (9), and (10).

#### IV. NUMERICAL METHOD: SPECTRAL DISCRETIZATION

Let  $\{\lambda_k, e_k\}_{k \geq 0}$  denote the eigenvalues and eigenfunctions of the operator  $\mathcal{H}$ . Without loss of generality, we reorder the eigenvalues as a non-decreasing sequence so that  $\lambda_0 = 0$  and  $\lambda_1 > 0$ . The eigenfunctions  $\{e_k\}_{k \geq 0}$  form a  $L^2(\mathbb{R}^d)$ -orthonormal basis. In particular, we have  $e_0 = \sqrt{\rho_\infty}$  since  $\rho_\infty$  is the steady state of equation (2).

The solution  $\psi(x, t)$  of equation (7) is expanded as

$$\psi(x, t) = \sum_{k=0}^{\infty} a_k(t) e_k(x).$$

Substituting this expansion into the equation (7) and projecting onto each  $e_i(x)$  yields the infinite system of ordinary differential equations (ODEs)

$$\dot{a}_i(t) = -\lambda_i a_i(t) + \sum_{j=1}^m u_j(t) \sum_{k=0}^{\infty} a_k(t) \langle \mathcal{N}_j e_k, e_i \rangle_{L^2(\mathbb{R}^d)} \quad (12)$$

Since  $\lambda_k \rightarrow \infty$  as  $k \rightarrow \infty$ , higher modes decay rapidly, which justifies the truncation of the expansion to a finite-dimensional system.

**Remark.** Notice that

$$\begin{aligned} a_0(t) &= \int_{\mathbb{R}^d} \psi(x, t) e_0(x) dx = \int_{\mathbb{R}^d} \psi(x, t) \sqrt{\rho_\infty(x)} dx \\ &= \int_{\mathbb{R}^d} \rho(x, t) dx = 1, \quad \forall t \geq 0. \end{aligned}$$

We check that  $\mathcal{N}_i^*[\sqrt{\rho_\infty}] = 0$  for each  $i = 1, \dots, m$  since  $b_i = \rho_\infty^{-1/2} \nabla \alpha_i \cdot \nabla \sqrt{\rho_\infty}$ . This relation implies that the controlled equation (12) satisfies  $\dot{a}_0(t) = 0$  for all  $t \geq 0$ .

Similarly, expanding  $\varphi(x, t) = \sum_{k=0}^{\infty} p_k(t) e_k(x)$  leads to

$$\begin{aligned} \dot{p}_i(t) &= \lambda_i p_i(t) - \sum_{j=1}^m u_j(t) \sum_{k=0}^{\infty} p_k(t) \langle \mathcal{N}_j^* e_k, e_i \rangle_{L^2(\mathbb{R}^d)} \\ &\quad + \kappa(a_i - \hat{a}_i), \end{aligned} \quad (13)$$

where  $\hat{a}_i$  are the spectral coefficients corresponding to  $\hat{\psi}$ . The optimal control is then given by

$$u_i(t) = \frac{1}{\nu} \sum_{j,k=0}^{\infty} a_j(t) p_k(t) \langle \mathcal{N}_i^* e_k, e_j \rangle_{L^2(\mathbb{R}^d)}. \quad (14)$$

Considering a truncation to  $N$  eigenmodes, we define the matrices  $B^i, A^i \in \mathbb{R}^{N \times N}$  by

$$B_{jk}^i := \langle b_i e_j, e_k \rangle_{L^2(\mathbb{R}^d)}, \quad A_{jk}^i := \langle \nabla \alpha_i \cdot \nabla e_j, e_k \rangle_{L^2(\mathbb{R}^d)}.$$

The resulting coupled finite-dimensional system is

$$\begin{cases} \dot{\mathbf{a}}(t) &= -\Lambda \mathbf{a}(t) + \sum_{j=1}^m u_j(t) (B^j - A^j) \mathbf{a}(t), \\ \dot{\mathbf{p}}(t) &= \Lambda \mathbf{p}(t) - \sum_{j=1}^m u_j(t) (B^j - (A^j)^T) \mathbf{p}(t) \\ &\quad + \kappa(\mathbf{a}(t) - \hat{\mathbf{a}}), \end{cases} \quad (15)$$

with initial and terminal conditions

$$a_i(0) = \langle \psi_0, e_i \rangle_{L^2(\mathbb{R}^d)}, \quad p_i(T) = \langle \psi^\dagger, e_i \rangle_{L^2(\mathbb{R}^d)} - a_i(T),$$

where  $\Lambda$  is a diagonal matrix such that  $\Lambda_{ii} = \lambda_{i-1}$  for  $i \in \{1, \dots, N\}$  and  $B^j$  matrices are symmetric.

**Remark.** When  $\psi^\dagger = \hat{\psi} = \sqrt{\rho_\infty}$ , i.e., the target state is the unique steady state, convergence is achieved provided that  $\sum_{i=1}^N a_i(t)^2 \rightarrow 0$  as  $t \rightarrow \infty$ , i.e. when all modes apart from the steady-state mode (associated with  $a_0$ ) decay to zero. Since modes corresponding to small eigenvalues  $\lambda_i$  decay more slowly, it is important to design the control to target and accelerate the decay of them.

Under the regularity assumptions on  $W$ , classical spectral convergence theory ensures that the projection error decays rapidly with the number of modes. In particular, the truncated expansion converges to  $\psi$  in the  $L^2$  norm at a rate that depends on the smoothness of  $\psi$  (see, e.g., [18]).

### A. The Iterative Method

To compute the optimal control numerically, we employ a gradient descent method applied to the coupled system (15). The space-discretization of the gradient (11) is given by

$$\nabla_{u_j} J := \nu u_j - \langle \mathbf{p}(t), (B^j - A^j) \mathbf{a}(t) \rangle_{\mathbb{R}^N}. \quad (16)$$

Using this gradient, we perform the following iterative procedure, outlined in Algorithm 1.

---

**Algorithm 1** Spectral control solver with reduced gradient and Barzilai–Borwein update

---

**Require:**  $tol > 0$ ,  $k_{\max}$ , initial control functions  $u_1^0(t), \dots, u_m^0(t)$  (and  $u_1^{-1}(t), \dots, u_m^{-1}(t)$  for BB), final time  $T$ , and a time grid  $t_{\text{eval}}$ .

- 1: **Initialize:**  $k \leftarrow 0$ .
- 2: **while**  $\|\nabla J(u^k)\| > tol$  and  $k < k_{\max}$  **do**
- 3:   **(1)** Compute state coefficients  $\mathbf{a}(t)$  at  $t_{\text{eval}}$  by solving (12) with controls  $u_1^k, \dots, u_m^k$  and initial condition  $\mathbf{a}(0)$ .
- 4:   **(2)** Compute adjoint coefficients  $\mathbf{p}(t)$  at  $t_{\text{eval}}$  by solving (13) with controls  $u_1^k, \dots, u_m^k$ , state  $\mathbf{a}(t)$ , and terminal condition  $\mathbf{p}(T) = \mathbf{a}^\dagger - \mathbf{a}(T)$ .
- 5:   **(3)** Evaluate the gradient  $\nabla J_{u_j}(u_j^k)$  as in (16) for each  $j \in \{1, \dots, m\}$ .
- 6:   **(4)** Compute the Barzilai–Borwein step size

$$\gamma_k = \frac{\sum_{j=1}^m \langle u_j^k - u_j^{k-1}, \nabla J_{u_j}(u_j^k) - \nabla J_{u_j}(u_j^{k-1}) \rangle}{\sum_{j=1}^m \left| \nabla J_{u_j}(u_j^k) - \nabla J_{u_j}(u_j^{k-1}) \right|^2}.$$

- 7:   **(5)** For each  $j = 1, \dots, m$ , update the control:

$$u_j^{k+1}(t) = u_j^k(t) - \gamma_k \nabla J_{u_j}(u_j^k(t)).$$

- 8:   **(6)** Update the control interpolants on  $t_{\text{eval}}$ .
  - 9:   **(7)** Set  $k \leftarrow k + 1$ .
  - 10: **end while**
  - 11: **return** Optimal controls  $u_1^k(t), \dots, u_m^k(t)$ , state coefficients  $\mathbf{a}(t)$ , and adjoint coefficients  $\mathbf{p}(t)$ .
- 

In our numerical implementation, the eigenfunctions  $\{e_k\}$  and corresponding eigenvalues  $\{\lambda_k\}$  of the operator  $\mathcal{H}$  are computed using a finite element approach implemented in Wolfram Mathematica via the built-in function `NDEigensystem` [13] under Dirichlet boundary conditions on a sufficiently large domain, ensuring that the potential  $W$  is large. Alternatively, spectral methods or neural network approaches (e.g., [14]) may be employed. Once the eigenfunctions are computed, we use a trapezoidal rule to numerically integrate and obtain the matrices  $B^i$  and  $A^i$  for  $i \in \{1, \dots, m\}$ .

In Algorithm 1, the forward and adjoint systems are integrated using a Runge–Kutta method of order 5(4) with a relative tolerance of  $1 \times 10^{-7}$  and an absolute tolerance of  $1 \times 10^{-9}$ . The BB step size is then computed following the formulation in [8]. For a detailed analysis of the Barzilai–Borwein update in infinite-dimensional settings, see [6]. Although alternative iterative methods (such as line searches with Wolfe conditions or the non-linear conjugate gradient

method with the Armijo condition) can be employed, the BB update was chosen for its simplicity and efficiency.

### B. Choice of the Shape Function

In our optimal control framework, we only optimize over the time-dependent controls  $u_i(t)$  while keeping the shape functions  $\alpha_i(x)$  fixed. These shape functions modulate the spatial distribution of the control input and can influence the spectral properties of the operator  $\mathcal{H} - u_i \mathcal{N}_i$ . In particular, a careful choice of  $\alpha_i$  can increase the spectral gap of the controlled operator, thereby accelerating the convergence of the system toward its steady state.

For the purpose of choosing the functions  $\alpha_i$ , we introduce the deviation variable  $y(x, t) = \psi(x, t) - \sqrt{\rho_\infty(x)}$  for every  $(x, t) \in \mathbb{R}^d \times \mathbb{R}_{\geq 0}$ . The deviation function  $y(x, t)$  satisfies

$$y_t = -\mathcal{H}y + \sum_{j=1}^m u_j \mathcal{N}_j y + \sum_{j=1}^m u_j \mathcal{B}_j, \quad (17)$$

where  $\mathcal{B}_j := \mathcal{N}_j \sqrt{\rho_\infty}$  represents the effect of the control on the steady state.

Motivated by the Lyapunov-based feedback strategy introduced in [9], we select the shape function  $\alpha_j \in L^2(\mathbb{R}^d)$  to align the control with the slowest decaying modes. Specifically, we choose  $\alpha_j$  such that

$$\mathcal{B}_j = e_j \implies \nabla \cdot (\rho_\infty \nabla \alpha_j) = \sqrt{\rho_\infty} e_j,$$

for  $j \in \{1, \dots, m\}$  the  $m$  slowest modes of the operator  $\mathcal{H}$ . This condition intuitively ensures that the control acts in the direction of the slowest decaying modes, which are typically the bottleneck for convergence. The above PDE has a unique solution in  $L^2(\mathbb{R}^d)$ . Moreover, by the smoothness of  $\rho_\infty$  and  $e_j$ , the solution  $\alpha_j$  is smooth as well [11].

Although we do not claim that this choice is optimal in any formal sense, it provides a practical means of enhancing the influence of the control on the dynamics. In practice, we approximate the solution of this PDE by projecting onto a finite-dimensional basis, i.e.,

$$\alpha_j(x) \approx \sum_{k=1}^N c_{j,k} e_k(x)$$

and then we solve the resulting linear system for  $c_{j,k}$ .

### C. Initialization of the Control Functions

Due to the inherent nonconvexity of the optimal control problem – both in its infinite-dimensional formulation and its finite-dimensional discretization – gradient-based methods are not guaranteed to find the global minimum. Such methods may become trapped in suboptimal local minima and exhibit slow convergence. Moreover, while the BB step size update accelerates convergence, it does not guarantee that the cost function decreases monotonically at each iteration. In addition, initializing the control functions as constant zero functions (i.e.,  $u_i \equiv 0$  for all  $i$ ) may yield a terminal state that is close to the desired one for some parameter choices, but not necessarily accelerating convergence. This behavior can limit the efficiency of the algorithm and not steer the iterative process toward the desired global minimum. Therefore, selecting

a well-informed initial guess for  $u_i(t)$  is relevant to speed up convergence and avoid settling near an undesired local minimum.

Our strategy for control initialization is based on the linearization of the system around the steady state. Specifically, we consider the linearized equation

$$y_t = -\mathcal{H}y + \sum_{j=1}^m u_j(t) \mathcal{B}_j,$$

as in equation (17). We then formulate an infinite-horizon cost functional

$$J_\infty(y, \mathbf{u}) := \frac{1}{2} \int_0^\infty \left[ \kappa \|y(\cdot, t)\|_{L^2(\mathbb{R}^d)}^2 + \nu |\mathbf{u}(t)|^2 \right] dt,$$

which admits an optimal solution of the form

$$u_j^*(t) = -\frac{1}{\nu} \langle \Pi y(\cdot, t), \mathcal{B}_j^* \rangle_{L^2(\mathbb{R}^d)},$$

where  $\Pi$  is the solution of the associated Riccati equation

$$-\mathcal{H}\Pi - \Pi\mathcal{H} - \frac{1}{\nu} \Pi \left( \sum_{j=1}^m \mathcal{B}_j^* \mathcal{B}_j \right) \Pi + \kappa \mathcal{I} = 0,$$

where  $\mathcal{I}$  is the identity operator on  $L^2(\mathbb{R}^d)$ . This Riccati equation admits a unique solution, providing a well-defined optimal feedback law.

We compute the feedback control  $u_j^*(t)$  using spectral discretization as in the previous sections. Since we built matrices  $\Lambda$ ,  $B^j$ , and  $A^j$  for the algorithm, we can use them to solve the Riccati equation, which is fast. This computed feedback is then used as an initial guess for the iterative gradient-based optimization algorithm from **Section IV-A**. Our numerical experiments indicate that this initialization accelerates convergence, reduces numerical approximation errors, and helps avoid convergence to suboptimal solutions.

## V. NUMERICAL EXPERIMENTS AND RESULTS

In this section, we illustrate the performance of the proposed spectral control solver (Algorithm 1) on two benchmark cases. For simplicity, we fix  $\sigma = 1$  in all experiments. The first example is the quadratic potential

$$V_1(x, y) = \frac{1}{2}(ax^2 + by^2).$$

The invariant measure for this potential is a Gaussian measure with an ill-conditioned (when  $b \ll a$ ) covariance matrix. This potential allows the analytical computation of the eigenvalues and eigenfunctions of the operator  $\mathcal{H}$ , using the Metafunne–Palaria–Priola theorem [16]. In fact, for non-negative integers  $m, n$ , the eigenvalues are given by  $\lambda_{m,n} = an + bm$ . Since the spectral gap is  $\min(a, b)$ , choosing a small value for either  $a$  or  $b$  results in slow convergence toward the steady state. We refer to such cases as ill-conditioned. The second example is the separable double-well potential

$$V_2(x, y) = (x^2 - c_x)^2 + (y^2 - c_y)^2.$$

which leads to metastable behavior, at low temperatures and, consequently, to slow convergence.

In all experiments, we set the final time  $T = 5$ , control regularization parameter  $\nu = 10^{-4}$ , and running cost regularization parameter  $\kappa = 5$ . The solution is approximated using  $N = 50$  eigenmodes, and the initial condition is chosen as a truncated Gaussian distribution centered at  $(-0.2, 0.5)$ . We considered 500 iterations for the gradient method. The  $L^2$ -norm of the gradient achieved a value between  $10^{-4}$  and  $10^{-3}$  in the experiments. All experiments were performed on a Mac equipped with an Apple M3 processor (8 cores) and 16 GB of memory.

Figure 1 illustrates the evolution of the error norm  $\|a(t) - a^\dagger\|_2$ , over time for the quadratic potential with  $a = 1$  and two choices of  $b$  ( $b = 0.05$  and  $b = 0.1$ ). The plot compares controlled dynamics (solid lines) with uncontrolled dynamics (dashed line), demonstrating that the optimal control strategy accelerates convergence even in the challenging case of  $b = 0.05$ . We notice a reduction of four orders of magnitude for both experiments. Four control functions were set to be optimized, which are depicted in Figure 2. The control signals are strongly active during the initial moments of the experiment, after which they decay as the system approaches the steady state, and the first four modes approach zero.

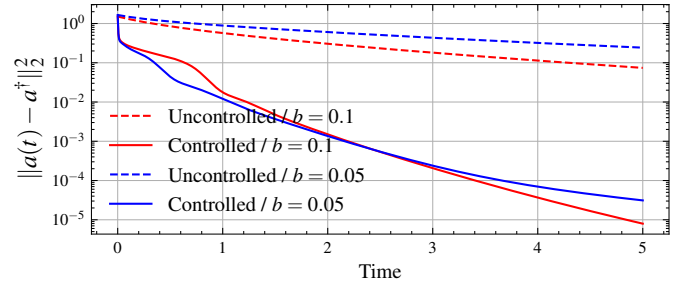


Fig. 1. Time evolution of the error norm for the quadratic potential with  $a = 1$  and  $b = 0.05, 0.1$ . The dashed lines represent the uncontrolled dynamics, while the undashed lines represent the controlled dynamics.

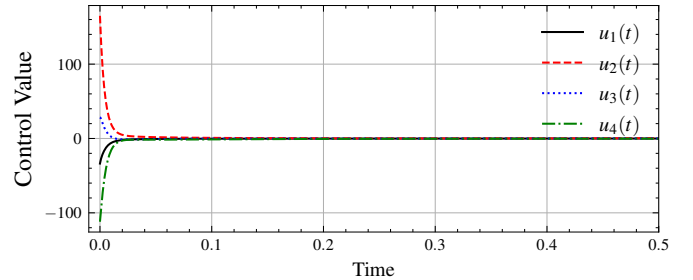


Fig. 2. The four optimized control functions for the quadratic potential experiments with  $a = 1$  and  $b = 0.1$ . We only consider the control up to time  $t = 0.5$  because, for  $t > 0.5$ , the control function remains close to zero.

Figure 3 presents the time evolution of the same error for the double-well potential. In the uncontrolled case (dashed curves), the error norm slowly decays because the system becomes temporarily trapped in one of the wells. In contrast, the optimal control strategy (solid curves) significantly

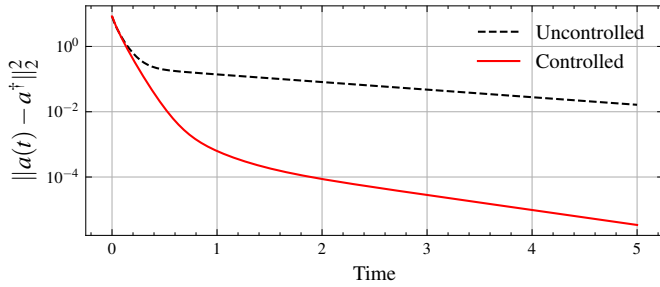


Fig. 3. Time evolution of the error norm for the double-well potential. The dashed line represents the uncontrolled dynamics, while the undashed one represents the controlled dynamics.

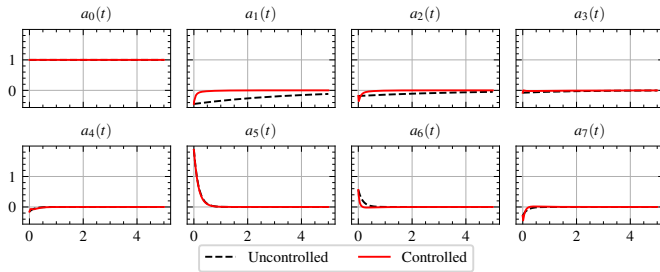


Fig. 4. Time evolution of the coefficients of the spectral decomposition of the double-well potential.

accelerates convergence, as evidenced by a steeper decay of the error, finishing with a final approximation error of three orders of magnitude less. The two control functions optimized for this example look similar to those of Figure 2. These results confirm that our spectral control approach is robust even for multimodal potentials, steering the system toward the desired steady state. Figure 4 compares the evolution of the coefficients under uncontrolled and controlled dynamics. In particular, the second and third components,  $a_1$  and  $a_2$ , are affected by the control, whereas others (e.g.,  $a_5$ ) remain essentially unchanged.

## VI. CONCLUSIONS

Our numerical experiments indicate that the proposed spectral control solver is effective in accelerating convergence to the desired steady state for both quadratic and double-well potentials. In particular, our results suggest that the slower-decaying modes (associated with small eigenvalues) are the primary targets of the control action when choosing the shape functions appropriately. Moreover, this framework can be applied to steer an initial distribution  $\rho_0$  toward a target  $\rho^\dagger$  that is different from the steady state, which is interesting for applications involving potentials with multiple local minima. Finally, the extension to higher dimensions strongly depends on solving the eigenvalue problem, computing the matrices  $A^j$  and  $B^j$ , and reliably approximating the solution using spectral modes.

## APPENDIX

We prove Proposition 1.

*Proof:* Applying the product rule to the definition of  $\mathcal{N}_i$  yields

$$\nabla \cdot (\sqrt{\rho_\infty} \phi \nabla \alpha_i) = \sqrt{\rho_\infty} \nabla \cdot (\phi \nabla \alpha_i) + \phi \nabla \sqrt{\rho_\infty} \cdot \nabla \alpha_i.$$

Dividing by  $\sqrt{\rho_\infty}$  and noting that

$$\frac{\nabla \sqrt{\rho_\infty}}{\sqrt{\rho_\infty}} = \nabla \log \sqrt{\rho_\infty},$$

we obtain

$$\mathcal{N}_i \phi = \nabla \cdot (\phi \nabla \alpha_i) + \phi \nabla \alpha_i \cdot \nabla \log \sqrt{\rho_\infty}.$$

This shows the desired expression. The formula for the formal adjoint follows from standard integration by parts. ■

## REFERENCES

- [1] A. Abdulle, G. A. Pavliotis, and U. Vaes. Spectral methods for multiscale stochastic differential equations. *SIAMASA J. Uncertain. Quantif.*, 5(1):720–761, 2017.
- [2] Giacomo Albi, Young-Pil Choi, Massimo Fornasier, and Dante Kalise. Mean field control hierarchy. *Applied Mathematics & Optimization*, 76:93–135, 2017.
- [3] M. P. Allen and D. J. Tildesley. *Computer Simulation of Liquids*. Oxford University Press, 2017.
- [4] M. Annunziato and A. Borzì. A Fokker-Planck control framework for stochastic systems. *EMS Surv. Math. Sci.*, 5(1-2):65–98, 2018.
- [5] M. S. Aronna and F. Troeltzsch. First and second order optimality conditions for the control of Fokker–Planck equations. *ESAIM Control Optim. Calc. Var.*, 27:15, 2021.
- [6] Behzad Azmi and Karl Kunisch. Analysis of the Barzilai-Borwein step-sizes for problems in Hilbert spaces. *Journal of Optimization Theory and Applications*, 185(3):819–844, 2020.
- [7] D. Bakry, F. Barthe, P. Cattiaux, and A. Guillin. A simple proof of the Poincaré inequality for a large class of probability measures including the log-concave case. *Electron. Commun. Probab.*, 13:60–66, 2008.
- [8] J. Barzilai and J. M. Borwein. Two-point step size gradient methods. *IMA J. Numer. Anal.*, 8(1):141–148, 1988.
- [9] T. Breiten, K. Kunisch, and L. Pfeiffer. Control strategies for the Fokker–Planck equation. *ESAIM Control Optim. Calc. Var.*, 24(2):741–763, 2018.
- [10] C. Castellano, S. Fortunato, and V. Loreto. Statistical physics of social dynamics. *Rev. Mod. Phys.*, 81(2):591–646, 2009.
- [11] D. Gilbarg and N. S. Trudinger. *Elliptic partial differential equations of second order*, pages 213–267. Springer US, 1997.
- [12] D. Helbing, A. Johansson, J. Mathiesen, M. H. Jensen, and A. Hansen. Analytical approach to continuous and intermittent bottleneck flows. *Phys. Rev. Lett.*, 97(16):168001, 2006.
- [13] Wolfram Research, Inc. *Mathematica*, Version 14.2. Champaign, IL, 2024.
- [14] H. Jin, M. Mattheakis, and P. Protopapas. Physics-informed neural networks for quantum eigenvalue problems. In *2022 Int. Joint Conf. Neural Netw. (IJCNN)*, pages 1–8. IEEE, 2022.
- [15] P. H. Jones, O. M. Maragò, and G. Volpe. *Optical Tweezers: Principles and Applications*. Cambridge University Press, Cambridge, 2015.
- [16] T. Lelièvre, F. Nier, and G. A. Pavliotis. Optimal non-reversible linear drift for the convergence to equilibrium of a diffusion. *J. Stat. Phys.*, 152(2):237–274, 2013.
- [17] J. L. Lions. *Optimal Control of Systems Governed by Partial Differential Equations*, volume 170. Springer, 1971.
- [18] M. Mohammadi and A. Borzì. A Hermite spectral method for a Fokker–Planck optimal control problem in an unbounded domain. *Int. J. Uncertainty Quantif.*, 5(3), 2015.
- [19] L. Pareschi and G. Toscani. Self-similarity and power-like tails in nonconservative kinetic models. *J. Stat. Phys.*, 124:747–779, 2006.
- [20] G. A. Pavliotis. *Stochastic Processes and Applications*, volume 60 of *Texts in Applied Mathematics*. Springer, 2014.
- [21] A. P. Peirce, M. A. Dahleh, and H. Rabitz. Optimal control of quantum-mechanical systems: Existence, numerical approximation, and applications. *Phys. Rev. A*, 37(12):4950, 1988.
- [22] M. Reed and B. Simon. *IV: Analysis of Operators*, volume 4. Elsevier, 1978.